Magnetic Resonance Materials in Physics, Biology and Medicine (2019) 32:519–527
https://doi.org/10.1007/s10334-019-00764-0

SHORT COMMUNICATION

Effect of combination and number of *b* values in IVIM analysis with post-processing methodology: simulation and clinical study

Archana Vadiraj Malagi[1] · Chandan J. Das[2] · Kedar Khare[3] · Fernando Calamante[5] · Amit Mehndiratta[1,4]

Received: 8 March 2019 / Revised: 10 May 2019 / Accepted: 4 June 2019 / Published online: 18 June 2019

Abstract

Objective To investigate the effect of number and combination of *b* values used on the accuracy of estimated Intravoxel Incoherent Motion (IVIM) parameters using simulation and clinical data.

Materials and methods Simulations with seven combinations of *b* values were performed for 4, 6, 8, and 13 numbers of *b* values with six different values of *D*, *D**, and *f* parameters. Two methodologies were implemented for IVIM analysis: standard biexponential model (BE) and biexponential model with total variation penalty function (BE + TV). Clinical data set of six patients with prostate cancer was retrospectively analyzed using 4, 8, and 13 *b* values.

Results BE + TV method showed lesser error and lower variability in simulation and clinical data, respectively. 8 and 13 *b* values showed good agreement in the values of parameters estimated with high correlation coefficient ($\rho = 0.83$–0.93). Clinical data showed high spurious noise with lower *b* values [4 *b* values leading to high coefficient of variation (CV); however, substantially, lower CV was observed with 8 and 13 *b* values].

Discussion BE model with TV penalty function is robust to combination of *b* values used for IVIM analysis. Combination of 8 *b* values provided a reasonably good accuracy in IVIM parameters.

Keywords Intravoxel incoherent motion · Diffusion-weighted imaging · Prostate cancer · *b* values · Total variation penalty function · Biexponential model

Introduction

Diffusion-weighted imaging (DWI) is an imaging sequence routinely used for lesion localization in prostate cancer patient with conventional MRI [1]. DWI signal is modelled using monoexponential function to obtain the apparent diffusion coefficient (ADC), a quantitative measure of water diffusion in tissues [2]. This monoexponential model is highly sensitive to water diffusion in extravascular extracellular space, i.e., when *b* values are greater than 200 s/mm^2.

A special type of DWI sequence, which is sensitive to both water diffusion in extravascular space and intravascular space (pseudo-perfusion) is called Intravoxel Incoherent Motion (IVIM) imaging, i.e., it can capture diffusion and perfusion information of the tissue region with no external contrast agent [3]. For IVIM, data are acquired with a range of *b* values, and typically modelled with a standard biexponential (BE) function:

$$\frac{S}{S_0} = fe^{-bD^*} + (1-f)e^{-(bD)}$$

to evaluate the IVIM parameters diffusion coefficient (*D*), pseudo-diffusion coefficient (*D**), and perfusion fraction (*f*) [3]. Currently, IVIM is not often used in clinical evaluation; reasons include lack of agreement regarding standard protocols (e.g., for prostate cancer imaging), and non-physiological noise in parameter maps generated using the standard BE model [3]. To address the latter, an improved analysis

✉ Amit Mehndiratta
amit.mehndiratta@keble.oxon.org

1 Centre for Biomedical Engineering, Indian Institute of Technology Delhi, Hauz Khas, New Delhi 110016, India

2 Department of Radio-Diagnosis, All India Institute of Medical Sciences, New Delhi, India

3 Department of Physics, Indian Institute of Technology Delhi, Hauz Khas, New Delhi 110016, India

4 Department of Biomedical Engineering, All India Institute of Medical Sciences, New Delhi, India

5 Sydney Imaging and School of Aerospace, Mechanical and Mechatronic Engineering, University of Sydney, Sydney, Australia

method was recently proposed, where BE model with total variation (TV) penalty function was used [4]. Physical motivation of TV is to homogenize the whole 2D image at once, unlike conventional optimization, which processes every voxel independently [5, 6]. In this study, optimization with TV was used, which balances any sudden change in parameter map iteratively, thereby reducing non-physiological noise and preserving edges of tissue in an image [6, 7].

BE model with TV penalty function was shown to give stable parameter and qualitatively better parametric maps based on simulated and clinical data for a given combination of *b* values [4]. However, it is necessary to understand how the selection of *b* values in IVIM acquisition could affect the estimation of IVIM parameters. A good analysis methodology should be robust to the combination of *b* values used in acquisition. In this study, simulations were performed using various combination and number of *b* values, and these results were validated using clinical data.

Materials and methods

Simulations

Three simulations were performed, with one IVIM parameter varied at a time, while the other two remained constant. For each set of simulation, a digital phantom with two-dimensional parameter map (matrix size: 64 × 64) was generated based on the literature [8]. Figure 1 shows the representative digital phantom for *f* parameter:

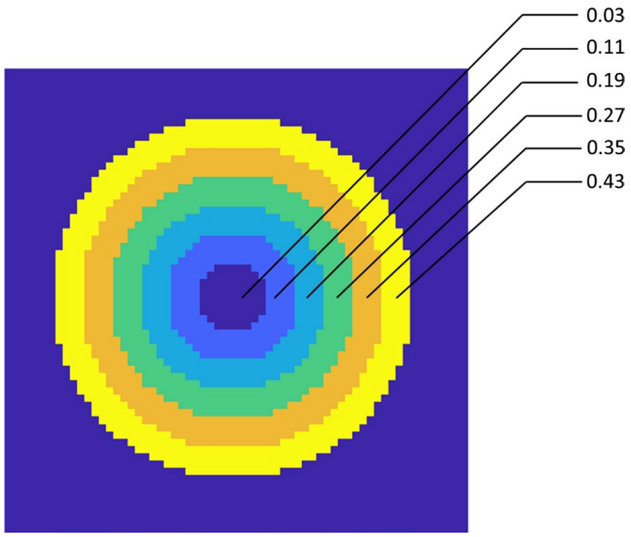

Fig. 1 Two-dimensional digital phantom with varying parameter map of *f* (matrix size: 64 × 64), consisting of concentric circles; *f* varied from 0.03 in center to 0.43 periphery, as indicated

Table 1 Different number and combinations of *b* values used in simulations

No. of *b* values	*b* value combinations (s/mm^2)
4 *b* values1	[0,25,200,2000]
4 *b* values2	[0,50,150,2000]
6 *b* values1	[0,25,100,800,1250,2000]
6 *b* values2	[0,50,150,500,1500,2000]
8 *b* values1	[0,25,75,100,200,800,1250,2000]
8 *b* values2	[0,50,75,150,500,800,1500,2000]
13 *b* values	[0,25,50,75,100,150,200,500,800 ,1000,1250,1500,2000]

$$\text{Simulation 1}: D = [0.7, 1.0, 1.3, 1.6, 1.9, 2.2] \times 10^{-3}\text{mm}^2/\text{s}; \quad D^* = 13 \times 10^{-3}\text{mm}^2/\text{s}; \quad f = 0.19;$$

$$\text{Simulation 2}: D = 1.3 \times 10^{-3}\text{mm}^2/\text{s}; D^* = [7, 10, 13, 16, 19, 22] \times 10^{-3}\text{mm}^2/\text{s}; \quad f = 0.19;$$

$$\text{Simulation 3}: D = 1.3 \times 10^{-3}\text{mm}^2/\text{s}; D^* = 13 \times 10^{-3}\text{mm}^2/\text{s}; \quad f = [0.03, 0.11, 0.19, 0.27, 0.35, 0.43];$$

Random Gaussian noise was added with SNR = 30 to each of the simulation sets. To evaluate the effect of number and combination of *b* values on estimated parameters, seven different combinations of *b* values were used, according to the literature [9] as shown in Table 1.

Only 4, 6, 8 and 13 *b* values were chosen in this study: 11–13 *b* values are commonly used in standard clinical routine for IVIM acquisition, having no difference in clinical interpretation [10, 11]; however, 4 *b* values have been suggested as optimal number for IVIM analysis in liver [9, 12]. For 4, 6, and 8 *b* values, two different combinations were used to evaluate the effect of combination of *b* values on parametric estimation. Fifty data sets (64 × 64 matrix each) were constructed for each simulation set with 7 different combinations of *b* values, leading to a total 4.3 million data sets simulated (64 × 64 × 50 × 3 × 7 = 4,300,800).

Clinical data acquisition

This study protocol was conducted with approval from Institutional review board and written consent from all patients was taken. Data set of six male patients with prostate cancer (63 ± 4.48 years) was acquired on a 1.5 T MRI (Achieva; Philips Healthcare, Best, The Netherlands) at the Department of Radiology, AIIMS, New Delhi, India, with a standard MRI protocol, including IVIM imaging with 13 *b* values = 0, 25, 50, 75, 100, 150, 200, 500, 800, 1000, 1250, 1500, 2000 s/mm^2 using phased-array surface coil (TR = 5.774 s, TE = 0.081 s).

4 and 8 *b* values' combinations were obtained by subsampling the 13 *b* values IVIM image. The clinical data was analyzed using the 4, 8 and 13 *b* values' combinations as used for the simulations (6 *b* values were not used in clinical data analysis, as it showed suboptimal results compared to 8 *b* values as elaborated in results).

Analysis of parameter map

Parameter estimation in simulation and clinical data was performed using in-house toolbox in MATLAB® (MathWorks Inc., v2016b, Philedellhia, PA, USA). All data sets were processed using both BE model and biexponential + TV model (BE + TV). Non-linear least square optimization was used for both BE and BE + TV. In BE + TV model, minimization of total variation was obtained, as shown in Eq. 1 [4, 7]:

$$\min_g f(g) = \min_g ||g - h||^2 + \alpha * TV(g). \tag{1}$$

TV(g) penalty is L1 norm of image gradient, as shown in Eq. 2 [5], where g and h are expected and observed image of size M × M, respectively. For every iteration, the image gradient was calculated and used to update the parameter values:

$$TV(g) = \sum_i \sqrt{\nabla_x g_x + \nabla_y g_y}. \tag{2}$$

Alpha is positive TV penalty parameter that balances between goodness of fit and data as measured by the optimizer, whereas beta is TV iteration stopping criterion. In this study, alpha and beta were set to 0.02 and 0.99, respectively [4, 7].

Error calculations

For simulations, relative root mean square error (RRMSE) was calculated for each parameter (D_{rrmse}, D^*_{rrmse}, and f_{rrmse}) in percentage as shown in Eq. 3, 4, 5:

$$\boldsymbol{D}_{\text{rrmse}} = \frac{\sqrt{\frac{\sum (D - D')^2}{N}}}{\overline{\boldsymbol{D}}} \times 100 \tag{3}$$

$$\boldsymbol{D}^*_{\text{rrmse}} = \frac{\sqrt{\frac{\sum \left(D^* - D^{*\prime}\right)^2}{N}}}{\overline{\boldsymbol{D}^*}} \times 100 \tag{4}$$

$$\boldsymbol{f}_{\text{rrmse}} = \frac{\sqrt{\frac{\sum (f - f')^2}{N}}}{\overline{\boldsymbol{f}}} \times 100, \tag{5}$$

where D', $D^{*\prime}$, and f' are estimated values, D, D^* and f are reference values, and $\overline{D}$, $\overline{D^*}$, and $\overline{f}$ are mean values, and N is total number of elements in reference map. RRMSE is a measure of accuracy: RRMSE = 0 represents a good accuracy.

For clinical data, coefficient of variation (CV), Spearman correlation coefficient (ρ), and Bland Altman plots were used to respectively assess the variations, associations, and agreements between parameters estimated using different combinations of *b* values.

Three regions of interests (ROI) of ~ 350 voxels were drawn on b = 2000 s/mm^2 image in every patient, a representative case presented in Fig. 2: (1) tumor region; (2)

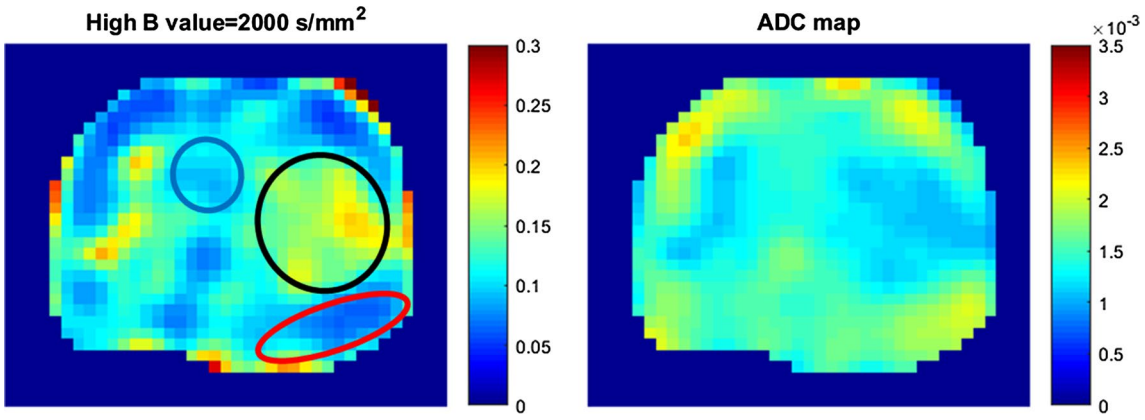

Fig. 2 Prostate cancer PIRADS 4 lesion in left transitional zone (Tz) appearing hyperintense on high *b* value IVIM image and hypointense on corresponding ADC map. Example ROIs, corresponding to tumor (black), and healthy tissue drawn on transition zone (blue) and peripheral zone (red)

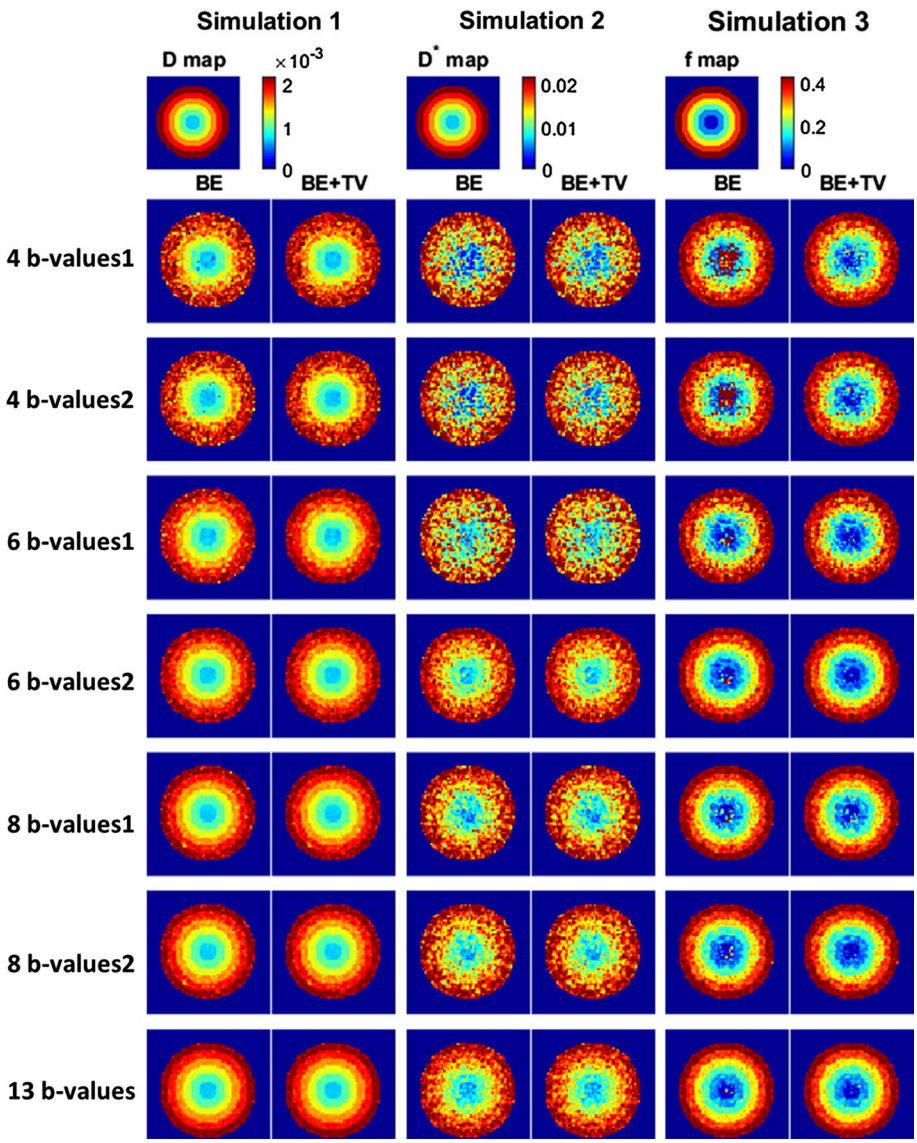

Fig. 3 Estimated parameter maps using various combinations of *b* values using BE and BE + TV for Simulations 1, 2 and 3. First row represents the *D, D**, and *f* reference maps

transition zone (Tz); and (3) peripheral zone (Pz) of prostate. For tumor ROI, high *b* value image (b = 2000 s/mm^2) and ADC map were used to localize the lesion by identifying a hyperintense region in high *b* value image and corresponding hypointense region present in ADC map. Wilcoxon signed-rank test was used for statistical comparison of estimated parameters between combinations of *b* values used in both simulations and clinical data.

Results

Simulations

Figure 3 shows estimated parameter with BE and BE + TV method using different combination of *b* values. Qualitatively parameter maps by BE were poor quality with high spurious values present as compared to BE + TV. Estimated *D* map quality was good as compared to other parameters for both methods and all combinations of *b* values. 8 *b* values' combinations and 13 *b* values showed similar estimated parameter maps. 4 and 6 *b* values' combinations showed higher noise in estimated parameters (especially for *D** and *f* parameter). Qualitatively, the parameter estimation improves with increasing the number of *b* values from 4 to 13.

Figure 4 shows bar plots of RRMSE in estimated parameters of all simulations. RRMSE broadly decreased with increasing number of *b* values. BE + TV method showed lower RRMSE by a factor of 15 ± 10% in parameter *D*, 3 ± 2% in parameter *D**, and 42 ± 16% in parameter *f* compared to BE across all combinations of *b* values. In all IVIM parameters estimated using BE+TV method, the improvement by TV penalty function was higher with lower number of *b* values (4 *b* values' combinations), with

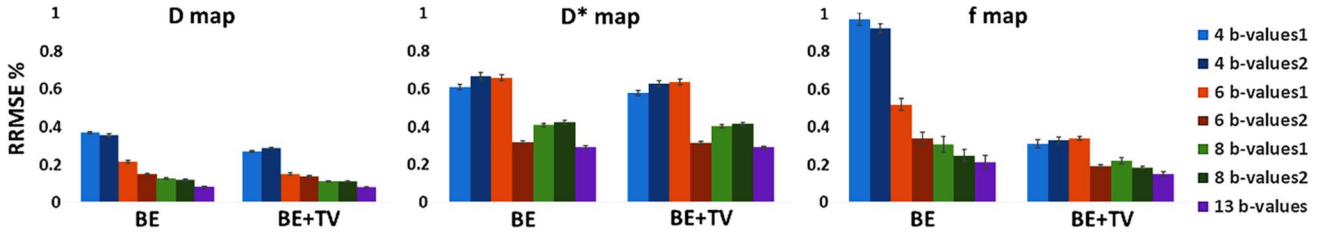

Fig. 4 Bar plots showing RRMSE of simulated *D* map, *D** map, and *f* map generated using different combinations of *b* values

reduced RRMSE. It was also observed that *f* parameter showed largest reduction in RRMSE by 42 ± 16% (across all *b* value combinations) with BE + TV method as compared to BE. RRMSE of both 8 *b* values' combinations showed similar trend as 13 *b* values for BE + TV method.

Clinical data

Mean values of estimated IVIM parameters for prostate using 4, 8, and 13 *b* values are shown in Table 2. Average *D* and *f* remained similar for any *b* value combinations or method used, whereas in *D**(BE), there was significant differences ($p < 0.05$) for 8 *b* values' combinations in tumor. Figure 5 shows the IVIM parametric maps for one representative patient with prostate cancer PIRADS 4, using different numbers of *b* values. Tumor appears hypointense in *D* map and hyperintense in *D** and *f* maps. Qualitatively, *D** map with 4 *b* values' combination appears noisy, whereas *D** and *f* map estimated with 8 and 13 *b* values, appears similar. Figure 6 shows the Bland–Altman plot of all IVIM parameters estimated using 8 and 13 *b* values with BE + TV method. For all parameters, the data points were within ± 2 SD interval and showed tight correlation among 8 and 13 *b* values ($\rho = 0.83$–0.93) except for *f* in Pz region. Figure 7 shows CV for parameters of tumor, Tz, and Pz regions. BE + TV consistently showed lower value of CV by 30–50% as compared to BE. BE + TV method was observed to be robust to different combinations of *b* values in both combinations of 4 or 8 *b* values; it had no significant differences for CV among two different combinations using 4 or 8 *b* values.

Discussion

It is important to determine the effect of number and combination of *b* values used in the estimation of IVIM parameters, in order to ensure that the methodology used is robust to *b* value combinations. Appropriate selection of *b* values is necessary for IVIM analysis in any clinical protocol, as it can directly impact acquisition time. The previous studies on *b* value optimization used only BE model [9, 13, 14] and other models such as segmented approach, stretched model, kurtosis model, etc. [15, 16]; however, the impact of post-processing methodologies was not investigated. Cohen et al. showed that perfusion-related parameters such as *D** and *f* are poorly estimated using BE model [17]. In our study, seven combinations of *b* values were evaluated using simulations and clinical data, and the analysis was performed using two methods (BE model and BE model with TV penalty function).

In this study, the overall SNR used in simulations was 30 and the total acquisition time was not kept constant. For all the simulations, the maximum *b* values used were 2000 s/mm^2, and thus, TE was assumed to be constant for all protocols [18]. In principle, it would be possible to simulate data with equal total acquisition time using a normalised SNR condition [19] (for example, comparing 12 *b* values vs. comparing three averages of 4 *b* values, i.e., with the same total effective SNR/time). However, such simulation would be appropriate when the intention is to see whether, for all other things being equal (particularly time and SNR), having more *b* values is beneficial (vs. having less *b* values, but repeatedly acquired). Instead, here, we seek to determine whether acquiring less data (and, therefore, with less overall SNR, but more importantly with less total acquisition time) comes at a large penalty on the quality of the resulting IVIM parameter maps. In line with the same objective for analysis of clinical data, we acquired clinical data with 13 *b* values and subsampled this set using different combinations of 4 *b* values and 8 *b* values for the analysis. Furthermore, as we kept the maximum *b* value = 2000 s/mm^2 same for all combinations used in simulations and clinical data, TE (and, therefore, base SNR) remained constant for all combinations.

In simulations, BE + TV showed accurate estimation for all parameters using any combinations of *b* values with at least 8 *b* values required for reliable estimation. Jambor et al. [20] have shown that 8–10 *b* values provide optimal results with overall less acquisition time in prostate, which is in accordance with our results. In addition, as the number of *b* values was increased, the RRMSE in *D* and *f* parameters decreased, for both BE and BE + TV method; however, the variance was much lower for BE + TV methods. Effect of TV was more prominent when there are fewer *b* values available for analysis. Thus, with fewer *b* values (poor SNR and

Table 2 ADC, D, D^*, and f (mean ± SD) values for tumor, transition zone, and peripheral zone in prostate using different combinations of b values

Tissue-type	Parameter	4 b values1		4 b values2		8 b values1		8 b values2		13 b values	
	ADC ($\times 10^{-3}$) mm^2/s	1.47 ± 0.45		1.46 ± 0.5		1.29 ± 0.3		1.32 ± 0.29		1.15 ± 0.24	
		BE	BE + TV	BE	BE + TV	BE	BE + TV	BE	BE + TV	BE	BE + TV
Tumor	D ($\times 10^{-3}$) mm^2/s	0.71 ± 0.16	0.82 ± 0.14	0.67 ± 0.21	0.8 ± 0.17	0.67 ± 0.18	0.77 ± 0.18	0.65 ± 0.18	0.76 ± 0.18	0.68 ± 0.2	0.8 ± 0.2
	D^* ($\times 10^{-3}$) mm^2/s	17.55 ± 3.72	17.87 ± 3.73	18.19 ± 5.64	16.6 ± 5.79	13.66 ± 4.3	7.17 ± 2.44	8.33 ± 2.09	6.48 ± 1.54	14.19 ± 4.69	11.02 ± 7.15
	f	0.33 ± 0.04	0.22 ± 0.03	0.33 ± 0.07	0.2 ± 0.03	0.44 ± 0.05	0.36 ± 0.05	0.44 ± 0.04	0.36 ± 0.04	0.41 ± 0.11	0.32 ± 0.04
	ADC ($\times 10^{-3}$) mm^2/s	2.36 ± 0.2		2.56 ± 0.5		2.07 ± 0.16		2.09 ± 0.14		1.7 ± 0.23	
		BE	BE + TV	BE	BE + TV	BE	BE + TV	BE	BE + TV	BE	BE + TV
Pz	D ($\times 10^{-3}$) mm^2/s	0.93 ± 0.12	1.09 ± 0.11	0.92 ± 0.13	1.09 ± 0.11	1.12 ± 0.25	1.22 ± 0.2	1.01 ± 0.14	1.18 ± 0.2	1.06 ± 0.25	1.24 ± 0.21
	D^* ($\times 10^{-3}$) mm^2/s	18.62 ± 8.95	18.5 ± 8.25	19.89 ± 11.48	18.22 ± 8.5	19.84 ± 10	8.78 ± 4.22	13.35 ± 9	7.02 ± 2.28	15.98 ± 5.37	11.61 ± 7.05
	f	0.41 ± 0.06	0.27 ± 0.02	0.53 ± 0.04	0.41 ± 0.06	0.47 ± 0.08	0.41 ± 0.06	0.53 ± 0.04	0.41 ± 0.06	0.41 ± 0.11	0.32 ± 0.04
	ADC ($\times 10^{-3}$) mm^2/s	1.91 ± 0.11		1.92 ± 0.15		1.61 ± 0.15		1.67 ± 0.13		1.42 ± 0.16	
		BE	BE + TV	BE	BE + TV	BE	BE + TV	BE	BE + TV	BE	BE + TV
Tz	D ($\times 10^{-3}$) mm^2/s	0.9 ± 0.11	1.02 ± 0.09	0.85 ± 0.15	1.01 ± 0.13	0.92 ± 0.13	1 ± 0.12	0.87 ± 0.1	0.99 ± 0.14	0.96 ± 0.13	1.04 ± 0.15
	D^* ($\times 10^{-3}$) mm^2/s	13.66 ± 1.62	14.44 ± 1.54	14.84 ± 2.4	13.94 ± 1.82	11.87 ± 4.37	6.13 ± 1.6	9.76 ± 1.67	5.72 ± 0.69	13.88 ± 3.73	10.05 ± 5.9
	f	0.37 ± 0.04	0.24 ± 0.02	0.39 ± 0.08	0.22 ± 0.03	0.45 ± 0.08	0.4 ± 0.06	0.48 ± 0.04	0.4 ± 0.04	0.39 ± 0.07	0.33 ± 0.02

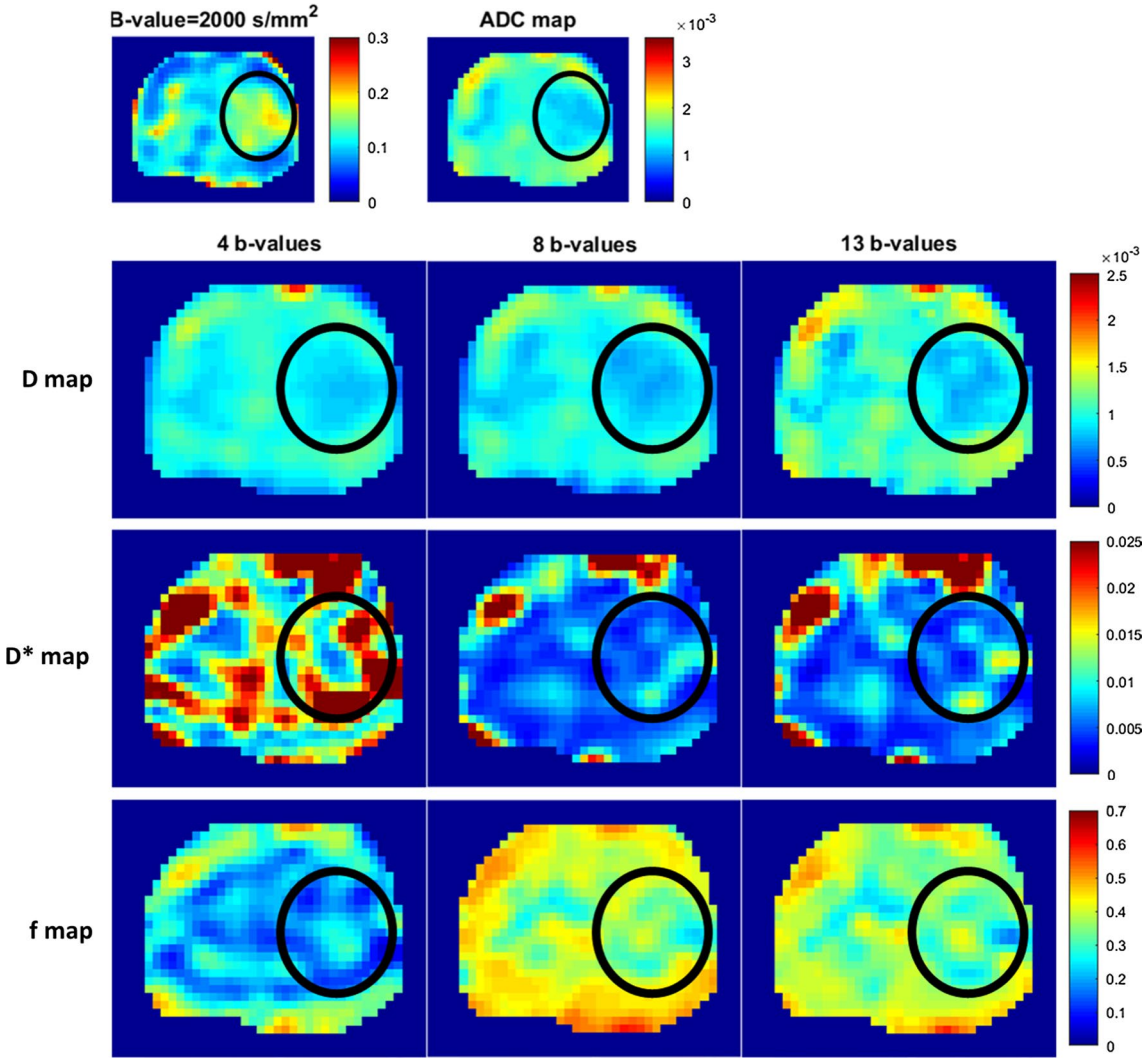

Fig. 5 Representative patient with prostate cancer PIRADS 4 lesion in left transitional zone (Tz) as shown as hyperintense in high *b* value image and hypointense in ADC map. IVIM parameter maps (*D*, *D**, *f*) using BE + TV using 4 *b* values1, 8 *b* values1, 13 *b* values; tumor is circled (Black) showing hypointense in *D* and hyperintense in *D** and *f*

shorter acquisition time), the quality of parameter estimation can be improved substantially with TV penalty function. Qualitatively, the error in estimation of parameters reduced with increasing number of *b* values. Also, it was expected that the error will be lower with increasing SNR. However, it was noticed that there is a non-linear decrease in RRMSE with increasing number of *b* values and with respect to SNR, which is specifically prominent for parameter *D**. The same has been reported earlier in the literature, *D** parameter is most susceptible to noise and shows poor reproducibility for low SNR [17, 21, 22]; there is also non-linear dependency of overall fit quality of parameters with SNR and combination of *b* values [13]. The *f* parameter map with BE showed less accuracy in any combinations, in comparison with *D* and *D** parameters. For both the combinations of 8 *b* values used, *D* parameter didn't show any differences while using BE+TV method, which suggests that BE + TV is insensitive to the specific combination for the same number of *b* values used.

CV was consistently lower for BE + TV compared to BE method, and Bland–Altman plot showed good agreement in estimated parameters using 8 and 13 *b* values with BE + TV method. Parametric image quality and parameter values show no difference among 8 and 13 *b* values when using BE + TV method, as shown in Fig. 5. The previous studies have suggested to use lesser *b* values for shorter acquisition time [9, 23]. However, in our study, higher error in simulation and poor image quality with higher CV in clinical data was observed when using 4 *b* values. Only two patients showed higher values of *D** in neurovascular bundle around prostate, which was not a consistent finding across patients. This would need to be further investigated for any potential clinical use. The study has few limitations, as, Gaussian

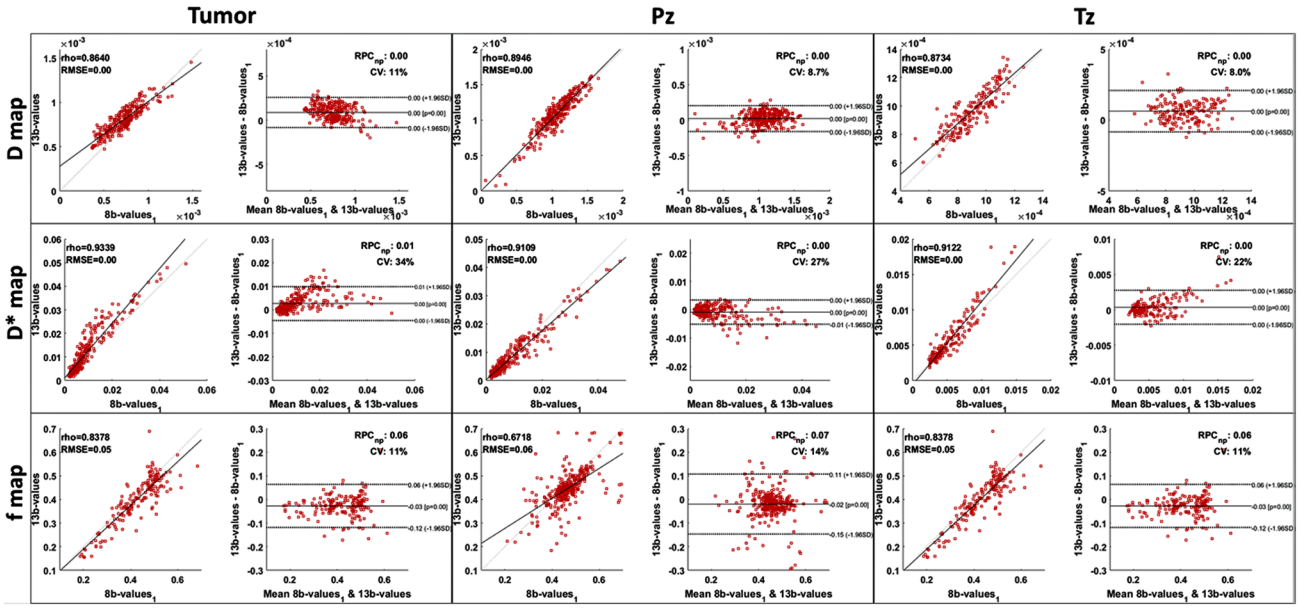

Fig. 6 Correlation and Bland–Altman plots of parameter generated from BE+TV using 8 *b* values1 and 13 *b* values in tumor, transition zone, and peripheral zone

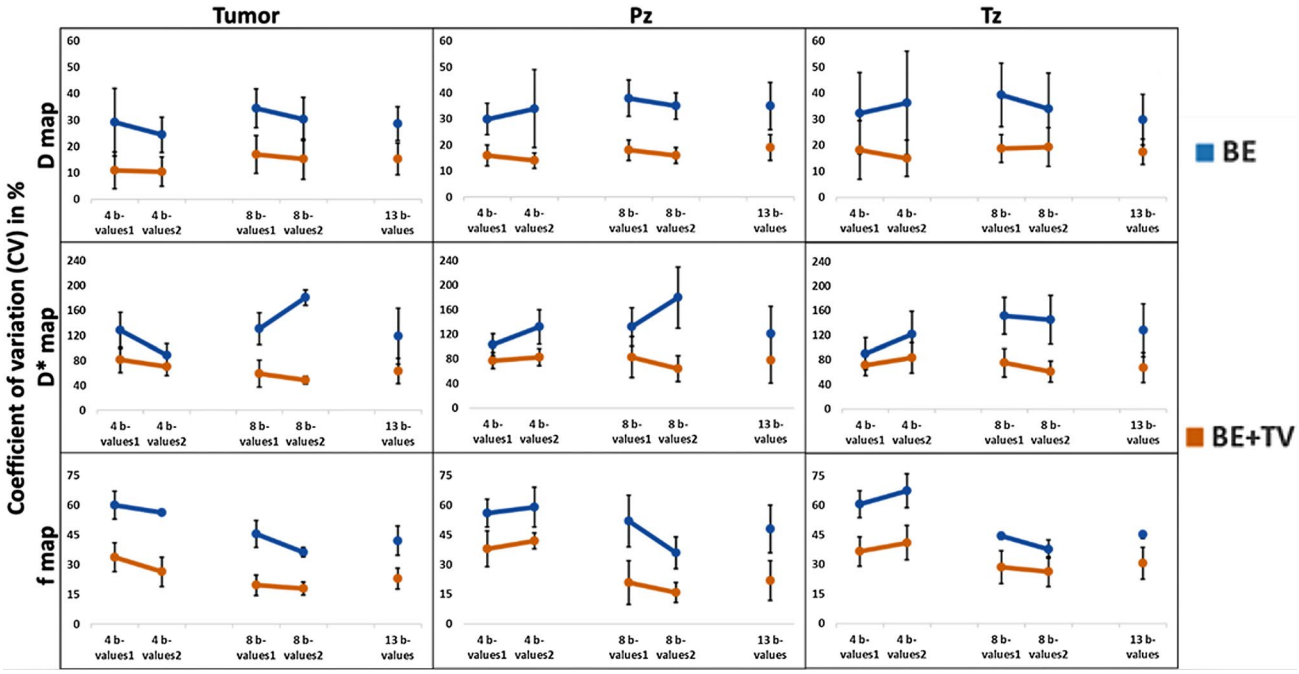

Fig. 7 Coefficient of variation (CV) of IVIM parameters *D* map, *D** map and *f* map generated from BE (blue) and BE+TV (orange) using 4, 8, and 13 *b* values

noise was used in the simulation; however, in literature use of Rician noise has been proposed [24], and this can be evaluated further. Sample size of clinical data was relatively small; in future, more data sets for optimization of *b* values could be evaluated.

In conclusion, a detailed analysis of post-processing methodology using biexponential and biexponential models with total variation penalty function has been performed. Biexponential model with total variation penalty function is robust to combinations of *b* values used

for IVIM analysis. Quality of perfusion fraction map is substantially improved with BE + TV method. 8 *b* values' acquisition with analysis using biexponential model with total variation penalty function provides a good practical compromise in terms of accuracy and acquisition time.

Acknowledgements Authors sincerely thank Ms. Esha Badiya Kayal for providing the codes of BE + TV algorithm and her support and mentorship in processing. The authors would like to acknowledge support staffs of IIT Delhi, New Delhi and AIIMS Delhi, New Delhi. A.V.M was supported with research fellowship, funded by Ministry of Human Resource Development, Government of India.

Authors' contributions AVM: study conception and design, acquisition of data, analysis and interpretation of data, drafting of manuscript, and critical revision. CJD: acquisition of data and analysis and interpretation of data. KK: analysis and interpretation of data. FC: analysis and interpretation of data, drafting of manuscript, critical revision. AM: study conception and design, analysis and interpretation of data, drafting of manuscript, critical revision.

Compliance with ethical standards

Conflict of interest All authors declare that he/she has no conflict of interest.

Ethical approval All procedures performed in studies involving human participants were in accordance with the ethical standards of the institutional and/or national research committee and with the 1964 Helsinki declaration and its later amendments or comparable ethical standards.

References

1. Haider MA, Van Der Kwast TH, Tanguay J, Evans AJ, Hashmi A-T, Lockwood G, Trachtenberg J (2007) Combined T2-weighted and diffusion-weighted MRI for localization of prostate cancer. AJR Am J Roentgenol 189:323–328
2. Stejskal EO, Tanner JE (1965) Spin diffusion measurements: spin echoes in the presence of a time-dependent field gradient. J Chem Phys 42:288–292
3. Le Bihan D, Breton E, Lallemand D, Aubin ML, Vignaud J, Laval-Jeantet M (1988) Separation of diffusion and perfusion in intravoxel incoherent motion MR imaging. Radiology 168:497–505
4. Kayal EB, Kandasamy D, Khare K, Alampally JT, Bakhshi S, Sharma R, Mehndiratta A (2017) Quantitative analysis of intravoxel incoherent motion (IVIM) diffusion MRI using total variation and huber penalty function. Med Phys 44:5849–5858
5. Rudin LI, Osher S, Fatemi E (1992) Nonlinear total variation based noise removal algorithms. Phys D 60:259–268
6. Vogel CR, Oman ME (1996) Iterative methods for total variation denoising. SIAM J Sci Comput 17:227–238
7. Sidky EY, Pan X (2008) Image reconstruction in circular cone-beam computed tomography by constrained, total-variation minimization. Phys Med Biol 53:4777
8. Shinmoto H, Tamura C, Soga S, Shiomi E, Yoshihara N, Kaji T, Mulkern RV (2012) An intravoxel incoherent motion diffusion-weighted imaging study of prostate cancer. AJR Am J Roentgenol 199:496–500
9. Dyvorne H, Jajamovich G, Kakite S, Kuehn B, Taouli B (2014) Intravoxel incoherent motion diffusion imaging of the liver: optimal b-value subsampling and impact on parameter precision and reproducibility. Eur J Radiol 83:2109–2113
10. Mazzoni LN, Lucarini S, Chiti S, Busoni S, Gori C, Menchi I (2014) Diffusion-weighted signal models in healthy and cancerous peripheral prostate tissues: comparison of outcomes obtained at different b-values. J Magn Reson Imaging 39:512–518
11. Beyhan M, Sade R, Koc E, Adanur S, Kantarci M (2018) The evaluation of prostate lesions with IVIM DWI and MR perfusion parameters at 3T MRI. Radiol Med 1–7.
12. Döpfert J, Lemke A, Weidner A, Schad LR (2011) Investigation of prostate cancer using diffusion-weighted intravoxel incoherent motion imaging. Magn Reson Imaging 29:1053–1058
13. Lemke A, Stieltjes B, Schad LR, Laun FB (2011) Toward an optimal distribution of b values for intravoxel incoherent motion imaging. Magn Reson Imaging 29:766–776
14. Zhang JL, Sigmund EE, Rusinek H, Chandarana H, Storey P, Chen Q, Lee VS (2012) Optimization of b-value sampling for diffusion-weighted imaging of the kidney. Magn Reson Med 67:89–97
15. Merisaari H, Jambor I (2015) Optimization of b-value distribution for four mathematical models of prostate cancer diffusion-weighted imaging using b values up to 2000 s/mm^2: simulation and repeatability study. Magn Reson Med 73:1954–1969
16. Cho GY, Moy L, Zhang JL, Baete S, Lattanzi R, Moccaldi M, Babb JS, Kim S, Sodickson DK, Sigmund EE (2015) Comparison of fitting methods and b-value sampling strategies for intravoxel incoherent motion in breast cancer. Magn Reson Med 74:1077–1085
17. Cohen AD, Schieke MC, Hohenwalter MD, Schmainda KM (2015) The effect of low b-values on the intravoxel incoherent motion derived pseudodiffusion parameter in liver. Magn Reson Med 73:306–311
18. Jones DK, Horsfield MA, Simmons A (1999) Optimal strategies for measuring diffusion in anisotropic systems by magnetic resonance imaging. Magn Reson Med An Off J Int Soc Magn Reson Med 42:515–525
19. Leporq B, Saint-Jalmes H, Rabrait C, Pilleul F, Guillaud O, Dumortier J, Scoazec J, Beuf O (2015) Optimization of intravoxel incoherent motion imaging at 3.0 Tesla for fast liver examination. J Magn Reson Imaging 41:1209–1217
20. Jambor I, Merisaari H, Aronen HJ, Järvinen J, Saunavaara J, Kauko T, Borra R, Pesola M (2014) Optimization of b-value distribution for biexponential diffusion-weighted MR imaging of normal prostate. J Magn Reson imaging 39:1213–1222
21. Andreou A, Koh DM, Collins DJ, Blackledge M, Wallace T, Leach MO, Orton MR (2013) Measurement reproducibility of perfusion fraction and pseudodiffusion coefficient derived by intravoxel incoherent motion diffusion-weighted MR imaging in normal liver and metastases. Eur Radiol 23:428–434
22. Pang Y, Turkbey B, Bernardo M, Kruecker J, Kadoury S, Merino MJ, Wood BJ, Pinto PA, Choyke PL (2013) Intravoxel incoherent motion MR imaging for prostate cancer: an evaluation of perfusion fraction and diffusion coefficient derived from different b-value combinations. Magn Reson Med 69:553–562
23. Meeus EM, Novak J, Dehghani H, Peet AC (2018) Rapid measurement of intravoxel incoherent motion (IVIM) derived perfusion fraction for clinical magnetic resonance imaging. Magn Reson Mater Phy 31:269–283
24. Gudbjartsson H, Patz S (1995) The rician distribution of noisy mri data. Magn Reson Med 34(6):910–914